第 33 卷第 5 期
2017 年 5 月

无 机 化 学 学 报
CHINESE JOURNAL OF INORGANIC CHEMISTRY

Vol.33 No.5
897-904

基于不对称三氮唑衍生物配体的三个配合物的制备、晶体结构及光催化性能

徐周庆[1] 何亚玲[1] 李慧军*,[1] 张培玲[2] 王 元*,[1] 王 奇[1] 钟润斌[1] 贾 磊*,[1]

([1]河南理工大学化学化工学院,焦作 454000)

([2]河南理工大学物理与电子信息学院,焦作 454000)

摘要: 利用水热法合成了基于不对称三氮唑衍生物配体 Hptp(Hptp=2-(5-(pyridin-3-yl)-1*H*-1,2,4-triazol-3-yl)pyrazine)的 3 个配合物 $[Cd_2(ptp)_2(SO_4)(H_2O)_2]_n$(**1**)、$[Zn(ptp)_2(H_2O)_2]$(**2**)和$[Cd(ptp)_2(H_2O)_2]$(**3**),它们的结构通过元素分析,红外,粉末 X 射线衍射和 X 射线单晶衍射表征。配合物 **1** 中,配体 ptp^-和 Cu^{2+}形成波浪状的一维结构,这些一维链通过 SO_4^{2-}链接形成三维结构。配合物 **2** 和 **3** 是同构化合物,单核单元在分子间氢键的作用下形成超分子二维平面。光催化降解实验表明,在双氧水存在时配合物 **1**~**3** 在 60 min 内使亚甲基蓝的降解率分别达到 79%、81%和 88%。

关键词: 三氮唑衍生物; 配合物; 光催化; 染料降解

中图分类号: O614.24+2; O614.24+1 **文献标识码**: A **文章编号**:1001-4861(2017)05-0897-08

DOI:10.11862/CJIC.2017.097

Three Coordination Complexes Based on an Asymmetric Triazole Derivative Ligand: Syntheses, Structures and Photocatalytic Properties

XU Zhou-Qing[1] HE Ya-Ling[1] LI Hui-Jun*,[1] ZHANG Pei-Ling[2]

WANG Yuan*,[1] WANG Qi[1] ZHONG Run-Bin[1] JIA Lei*,[1]

([1]*College of Chemistry and Chemical Engineering, Henan Polytechnic University, Jiaozuo, Henan* 454000, *China*)

([2]*College of Physics and Electronic Information, Henan Polytechnic University, Jiaozuo, Henan* 454000, *China*)

Abstract: Three coordination complexes, namely $[Cd_2(ptp)_2(SO_4)(H_2O)_2]_n$ (**1**), $[Zn(ptp)_2(H_2O)_2]$ (**2**) and $[Cd(ptp)_2(H_2O)_2]$ (**3**) (Hptp=2-(5-(pyridin-3-yl)-1*H*-1, 2, 4-triazol-3-yl)pyrazine), have been synthesized and characterized by elemental analyses, infrared spectra and single-crystal X-ray diffraction analyze. In complex **1**, corrugated 1D chains constructed by the ptp^- and Cd^{2+} were connected by SO_4^{2-} to form a 3D structure. In isostructural complexes **2** and **3**, intermolecular O-H ··· N hydrogen bonds link the mononuclear molecules into plane superstructure. The photocatalytic experiment result indicates that in the presence of H_2O_2, the degradation ratios of methylene blue (MB) reach to 79%, 81% and 88%, respectively, when complexes **1**, **2** and **3** act as catalyst. CCDC: 1487968, **1**; 1487969, **2**; 1487970, **3**.

Keywords: triazole derivative; complex; photocatalytic degradation

The study of coordination complexes has attracted great attentions in the last two decades due not only to their tunable structures, multiple topologies, but to their potential applications in many

收稿日期:2016-12-08。收修改稿日期:2017-03-13。

国家自然科学基金(No.U1604124,21404033,21401046)、河南省科技攻关项目(No.152102210314)、河南省高等学校重点科研项目(No.16A150010)和河南理工大学博士基金(No.72103/001/103)资助。

*通信联系人。E-mail:lihuijunxgy@hpu.edu.cn, wangyuan08@hpu.edu.cn,jlxj@hpu.edu.cn

areas such as fluorescent, adsorption and catalytic properties [1-4]. A new emerging application of coordination complexes is photocatalysis, and some results have demonstrated that coordination complexes are efficient photocatalysts on the degradation of organic dyes, water splitting, or photoreduction of CO_2 [5-7]. How to achieve inexpensive, stable, efficient, and band-gaptunable photocatalysts based coordination complexes is still a big challenge.

Generally, the properties of coordination complexes are mainly influenced by several factors, including organic linkers, centre metal ions, pH value, the solvent system and temperature [8-11]. Because the ligand could adopt different conformations and alternative linking modes in the crystallization, the rational selection of ligand always plays crucial role in the construction of the targeted coordination complexes. The triazole ligands offer different charge balance requirements, alternative linking modes, and orientation of donor groups which makes them have the potentiality to function as building units of structural topology [12-15]. Furthermore, we think that triazole derivatives should be a kind of appropriate ligand to construct novel coordination complexes with unique structure characters and interesting properties.

Motivated by the above-mentioned facts, 2-(5-(pyridin-3-yl)-1*H*-1,2,4-triazol-3-yl)pyrazine (Hptp), an asymmetric triazolate derivative which contains two potential bidentate chelating sites and two monodentate ones, may be a good candidate because the multiple N atoms facilitate the construction of coordination complexes. Herein, we employed Hptp and transitional metal salts to achieve three coordination complexes $[Cd_2(ptp)_2(SO_4)(H_2O)_2]_n$ (**1**), $[Zn(ptp)_2(H_2O)_2]$ (**2**) and $[Cd(ptp)_2(H_2O)_2]$ (**3**).

1 Experimental

1.1 Materials and measurements

All chemicals were commercially purchased except for Hptp which was synthesized according to the literature [16]. Elemental analyses for carbon, hydrogen and nitrogen were performed on a Thermo Science Flash 2 000 element analyzer. FTIR spectra were obtained in KBr disks on a PerkinElmer Spectrum One FTIR spectrophotometer in 4 000~450 cm^{-1} spectral range. Diffuse reflectance data were collected using a Shimadzu UV-3600 spectrophotometer, and the Kubelka-Munk function was used to estimate the optical band gap. The powder X-ray diffraction (PXRD) studies were performed with a Bruker AXS D8 Discover instrument (Cu $K\alpha$ radiation, λ=0.154 184 nm, U=40 kV, I=40 mA,) over the 2θ range of 5°~50° at room temperature.

1.2 Preparations of the complexes 1~3

1.2.1 Preparation of $[Cd_2(ptp)_2(SO_4)(H_2O)_2]_n$ (**1**)

A mixture of Hptp (0.05 mmol, 11.2 mg), $CdSO_4 \cdot 8/3H_2O$ (0.10 mmol, 25.6 mg), absolute ethanol (5 mL) and H_2O (5 mL) was placed in a Teflon-lined stainless steel vessel (25 mL), heated to 160 ℃ for 3 days, and then cooled to room temperature at a rate of 5 ℃·h^{-1}. Yellow block crystals of **1** were obtained and picked out, washed with distilled water and dried in air. Yield: 30.1 mg, 75% (based on Hptp). Elemental analysis Calcd. for $C_{22}H_{18}N_{12}O_6SCd_2$ (%): C32.89, H 2.26, N 20.92; Found (%): C 32.85, H 2.18, N 20.88. IR (KBr,cm^{-1}): 3 437, 3 004, 1 535, 1 497, 1 463, 1 406, 1 144.

1.2.2 Preparation of $[Zn(ptp)_2(H_2O)_2]$ (**2**)

A mixture of Hptp (0.05 mmol, 11.2 mg), $Zn(NO_3)_2 \cdot 6H_2O$ (0.1 mmol, 29.7 mg), absolute ethanol (8 mL) and CH_3CN (2 mL) was placed in a sealed flask (25 mL), heated to 160 ℃ for 3 days. Yellow block crystals of **2** were obtained and picked out, washed with distilled water and dried in air. Yield: 18.6 mg, 68 % (based on Hptp). Elemental analysis Calcd. for $C_{22}H_{18}N_{12}O_2Zn$ (%): C 48.23, H 3.31, N 30.68; Found (%): C 48.18, H 3.12, N 30.54. IR (KBr,cm^{-1}): 3 437, 2 968, 1 533, 1 494, 1 451, 1 413, 1 144.

1.2.3 Preparation of $[Cd(ptp)_2(H_2O)_2]$ (**3**)

The same prepared procedure as that for **2** was employed for **3** except that using $Cd(NO_3)_2 \cdot 4H_2O$ instead of $Zn(NO_3)_2 \cdot 6H_2O$. Yellow crystals of **3** were obtained and picked out, washed with distilled water and dried in air. Yield: 17.8 mg, 60% (based on Hptp). Elemental analysis Calcd. for $C_{22}H_{18}N_{12}O_2Cd$ (%): C 44.42, H 3.05, N 28.25; Found(%): C 44.38, H

2.98, N 28.21. IR (KBr, cm^{-1}): 3 437, 2 962, 1 531, 1 494, 1 451, 1 415, 1 144.

1.3.1 X-ray crystallography

X-ray single-crystal diffraction analysis of **1**~**3** was carried out on a Bruker SMART APEX Ⅱ CCD diffractometer equipped with a graphite monochromated Mo $K\alpha$ radiation (λ=0.071 073 nm) by using φ-ω scan technique at room temperature. The structures were solved via direct methods and successive Fourier difference synthesis (SHELXS-97)[17], and refined by the full-matrix least-squares method on F^2 with anisotropic thermal parameters for all non-H atoms (SHELXL-97). The empirical absorption corrections were applied by the SADABS program[18]. The H-atoms of carbon were assigned with common isotropic displacement factors and included in the final refinement by the use of geometrical restraints. H-atoms of water molecules were first located by the Fourier maps and then refined by the riding mode. The crystallographic data for complexes **1**~**3** are listed in Table 1. Moreover, the selected bond lengths and bond angles are listed in Table 2.

CCDC: 1487968, **1**; 1487969, **2**; 1487970, **3**.

Table 1 Crystal data and structural refinement of complexes 1~3

Complex	**1**	**2**	**3**
Empirical formula	$C_{22}H_{18}Cd_2N_{12}O_6S$	$C_{22}H_{18}N_{12}O_2Zn$	$C_{22}H_{18}N_{12}O_2Cd$
Formula weight	803.34	547.85	594.88
Temperature /K	296	296	296
Crystal system	Orthorhombic	Monoclinic	Monoclinic
Space group	*Pccn*	$P2_1/c$	$P2_1/c$
a / nm	1.329 18(14)	0.859 71(9)	0.863 4(5)
b / nm	2.023 6(2)	0.572 77(6)	0.569 9(3)
c / nm	0.988 50(11)	2.231 8(3)	2.316 7(13)
β / (°)	90	100.632(2)	99.013(8)
Volume / nm^3	2.658 8(5)	1.080 1(2)	1.125 8(11)
Z	4	2	2
D_c / ($g\cdot cm^{-3}$)	2.007	1.685	1.755
Absorption coefficient / mm^{-1}	1.753	1.190	1.020
F(000)	1576	560	596
Crystal size / mm	0.3×0.2×0.2	0.3×0.2×0.1	0.3×0.2×0.1
R_{int}	0.063 5	0.024 8	0.026 8
Reflections collected	12 632	5 243	4 369
Independent reflections	2 339	1 903	1 977
Goodness-of-fit on F^2	0.923	1.060	1.031
Final *R* indices [$I>2\sigma(I)$]	R_1=0.027 7	R_1=0.028 0	R_1=0.024 6
	wR_2=0.057 9	wR_2=0.066 4	wR_2=0.064 8
R indices (all data)	R_1=0.040 9	R_1=0.034 6	R_1=0.031 4
	wR_2=0.062 0	wR_2=0.069 3	wR_2=0.068 8

Table 2 Selected bond lengths (nm) and angles (°) for complexes 1~3

Complex **1**					
Cd(1)-O(1)	0.225 03(15)	Cd(1)-N(3)	0.231 50(16)	Cd(1)-O(3)	0.233 70(14)
Cd(1)-O(2)^i	0.228 12(14)	Cd(1)-N(6)^i	0.232 48(17)	Cd(1)-N(1)	0.247 07(17)
O(1)-Cd(1)-O(2)^i	96.38(6)	N(3)-Cd(1)-N(6)^i	115.75(6)	O(1)-Cd(1)-N(1)	77.88(5)

Continued Table 2

O(1)-Cd(1)-N(3)	147.95(5)	O(1)-Cd(1)-O(3)	95.60(5)	O(2)^{i}-Cd(1)-N(1)	86.66(5)
O(2)^{i}-Cd(1)-N(3)	89.06(5)	O(2)^{i}-Cd(1)-O(3)	167.88(5)	N(3)-Cd(1)-N(1)	70.92(6)
O(1)-Cd(1)-N(6)^{ii}	94.26(5)	N(3)-Cd(1)-O(3)	81.75(5)	N(6)^{ii}-Cd(1)-N(1)	169.75(5)
O(2)^{i}-Cd(1)-N(6)^{ii}	100.89(5)	N(6)^{ii}-Cd(1)-O(3)	76.34(5)	O(3)-Cd(1)-N(1)	97.68(5)
		Complex **2**			
Zn(1)-O(1)^{i}	0.210 82(15)	Zn(1)-O(1)	0.210 82(15)	Zn(1)-N(3)^{i}	0.216 63(17)
Zn(1)-N(3)	0.216 63(17)	Zn(1)-N(1)	0.218 35(17)	Zn(1)-N(1)^{i}	0.218 35(17)
O(1)^{i}-Zn(1)-O(1)	180.00(7)	N(3)^{i}-Zn(1)-N(3)	180.00(8)	O(1)^{i}-Zn(1)-N(1)^{i}	86.84(6)
O(1)^{i}-Zn(1)-N(3)^{i}	89.23(6)	O(1)^{i}-Zn(1)-N(1)	93.16(6)	O(1)-Zn(1)-N(1)^{i}	93.16(6)
O(1)-Zn(1)-N(3)^{i}	90.77(6)	O(1)-Zn(1)-N(1)	86.84(6)	N(3)^{i}-Zn(1)-N(1)^{i}	77.89(6)
O(1)^{i}-Zn(1)-N(3)	90.77(6)	N(3)^{i}-Zn(1)-N(1)	102.11(6)	N(3)-Zn(1)-N(1)^{i}	102.11(6)
O(1)-Zn(1)-N(3)	89.23(6)	N(3)-Zn(1)-N(1)	77.89(6)	N(1)-Zn(1)-N(1)^{i}	180.00(4)
		Complex **3**			
Cd(1)-O(1)^{i}	0.2312(2)	Cd(1)-N(3)	0.2331(2)	Cd(1)-N(1)	0.2401(2)
Cd(1)-O(1)	0.2312(2)	Cd(1)-N(3)^{i}	0.2331(2)	Cd(1)-N(1)^{i}	0.2401(2)
O(1)^{i}-Cd(1)-O(1)	180.00(8)	N(3)-Cd(1)-N(3)^{i}	180.00(9)	O(1)^{i}-Cd(1)-N(1)^{i}	87.33(7)
O(1)^{i}-Cd(1)-N(3)	91.28(8)	O(1)^{i}-Cd(1)-N(1)	92.67(7)	O(1)-Cd(1)-N(1)^{i}	92.67(7)
O(1)-Cd(1)-N(3)	88.72(8)	O(1)-Cd(1)-N(1)	87.33(7)	N(3)-Cd(1)-N(1)^{i}	107.10(8)
O(1)^{i}-Cd(1)-N(3)^{i}	88.72(8)	N(3)-Cd(1)-N(1)	72.90(8)	N(3)^{i}-Cd(1)-N(1)^{i}	72.90(8)
O(1)-Cd(1)-N(3)^{i}	91.28(8)	N(3)^{i}-Cd(1)-N(1)	107.10(8)	N(1)-Cd(1)-N(1)^{i}	180.00(4)

Symmetry codes: ^{i} x, $-y$+3/2, z+1/2; ^{ii} x−1/2, $-y$+1, $-z$+3/2 for **1**; ^{i} $-x$+1/2, $-y$+1/2, $-z$ for **2**; ^{i} $-x$, $-y$+1, $-z$ for **3**.

1.4 Photocatalytic experiments

To evaluate the photocatalytic activities of these three complexes, the photocatalytic degradation of methylene blue (MB) aqueous solution was performed at ambient temperature. The procedure was as follows: 30 mg of the desolvated samples was dispersed into 100 mL of methylene blue aqueous solution (12.75 mg·L^{-1}), followed by the addition of four drops of hydrogen peroxide solution (H_2O_2, 30%). The suspensions were magnetically stirred in the dark for over 1 h to ensure adsorption equilibrium of methylene blue onto the surface of samples. A 300 W xenon arc lamp was used as a light source. An optical filter in the equipment of xenon arc lamp was used to filtering out the UV emission below 400 nm. Then the above solutions were irradiated for 0, 20, 40, 60 and 80 min, and the corresponding reaction solutions were filtered and the absorbance of methylene blue aqueous solutions was then measured by a spectrophotometer. The characteristic peak (λ=665 nm) for MB was employed to monitor the photocatalytic degradation process. For comparison, the contrast experiment was completed under the same conditions without any cat alyst.

2 Results and discussion

2.1 Crystal structures of complexes 1~3

Single-crystal X-ray measurement reveals that complex **1** crystallizes in the orthorhombic space group *Pccn* and its asymmetric unit consists of one Cd(Ⅱ), one ptp^{-}, one half of SO_4^{2-} anion and one coordinated water. As shown in Fig.1a, the Cd1 ion is coordinated by three N atoms from two ptp^{-}, two oxygen atoms from two SO_4^{2-} and one coordinated water molecule, thus creating the distorted octahedron coordination geometry. The ptp^{-} indeed coordinates to two Cd(Ⅱ) ions from a chelating and a bridging site. The Cd-O bond distances are in the range of 0.202 81(14)~0.233 70(14) nm, and the Cd-N bond length is in the range of 0.231 50(16)~ 0.247 07(17)

nm. The Cd(Ⅱ) ions are connected by the ptp⁻ to form an interesting corrugated 1D chain (Fig.1b). We are gratified to note that each SO_4^{2-} in 1 connects four Cd (Ⅱ) adopting a $\mu_4,\eta^1\eta^1\eta^1\eta^1$-coordination mode. In this way, neighboring chains are connected by SO_4^{2-} to form the 3D structure of **1** (Fig.1c and 1d).

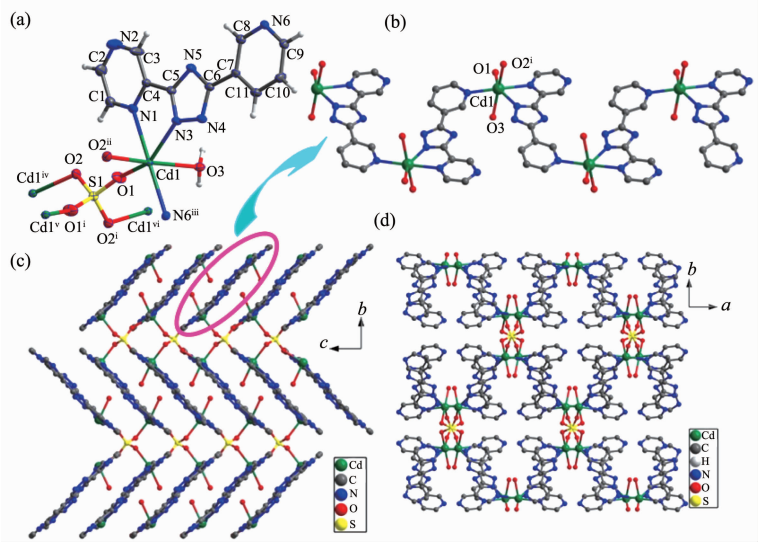

Symmetry codes: [i] 0.5−*x*, 1.5−*y*, *z*; [ii] *x*, 1.5−*y*, 0.5+*z*; [iii] −0.5+*x*, 1−*y*, 1.5−*z*; [iv] *x*, 1.5−*y*, −0.5+*z*; [v] 0.5−*x*, 1.5−*y*, *z*; [vi] 0.5−*x*, *y*, −0.5+*z*

Fig.1 View of ORTEP drawing of **1** with 30% thermal ellipsoids(a), zigzag 1D chain (b), 3D structure viewed from a axis(c), 3D structure viewed from *c* axis (d) in **1**

Single crystal X-ray diffraction analysis reveals that complexes **2** and **3** are isostructural and crystallize in the monoclinic system, space group $P2_1/c$ (Table 1). The structure of **2** will be discussed in detail as an example. The asymmetric unit of **2** consists of one half of Zn(Ⅱ), one ptp⁻ and one coordinated water molecule. As shown in Fig.2a, the Zn(Ⅱ) possesses a distorted octahedral coordination environment built by four N atoms from two ptp⁻ and two oxygen atom from coordinated water molecules (Zn-N 0.216 63(17)~0.218 35(17) nm, Zn-O 0.210 82(15) nm).

In the crystal of **2**, intermolecular O-H ⋯ N hydrogen bonds (O1-H1B⋯N6^{i} and O1-H1B⋯N4^{ii}, with D⋯A distances of 0.273 6(2) and 0.277 0(2) nm, D-H⋯A angles of 162.4° and 167.9°, respectively) link the complex molecules into plane structure, which is similar to the crystal of **3** except that the D⋯A distances are 0.274 2(3) and 0.277 5(3) nm and D-H ⋯ A angles are 160.3° and 173.0° (Fig.2b), respectively.

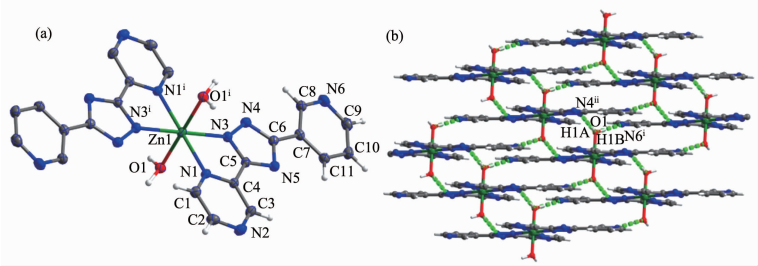

Fig.2 View of ORTEP drawing of **2** with 30% thermal ellipsoids (a) and 3D supramolecular architecture connected by hydrogen bonds in **2**(b)

2.2 Photocatalysis property

The powder X-ray diffraction (PXRD) patterns for three new complexes are presented in Fig.3, and each experimental pattern is almost same as the simulated pattern, except for a little difference about reflection intensities, which manifests that three new complexes are the purity phase.

The band gaps of complexes **1**~**3** were measured

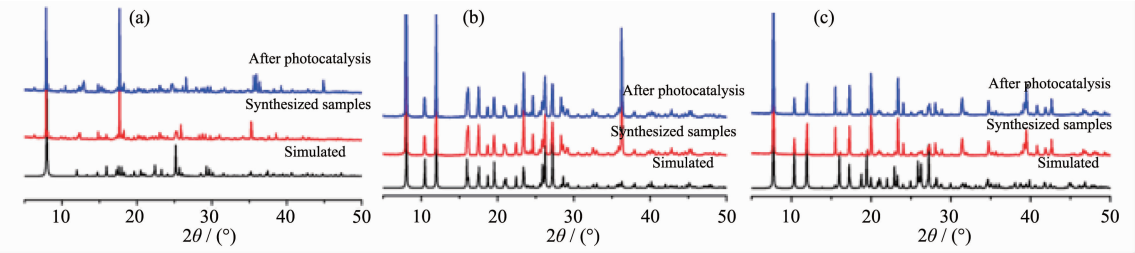

Fig.3 Powder XRD patterns for complexes **1**(a), **2**(b) and **3**(c)

by a solid state ultraviolet-visible (UV-Vis) diffuse reflection measurement method at room temperature. In a plot of K-M function versus energy, the band gap E_g is defined as the intersection point among the energy axis and line extrapolated of the linear portion[19]. The K-M function, $F=(1-R)^2/(2R)$ (R is the reflectance of an infinitely thick layer at a given wavelength), can be converted from measured diffuse reflectance data. As shown in Fig.4, the E_g values for complexes **1**~**3** are 1.85, 1.92 and 1.65 eV, respectively. The reflectance spectra show that there exist the optical band gap and semiconductive behaviors in complexes **1**~**3**, and these complexes can be employed as potential semiconductive materials (The E_g of a semiconductor is 1~3 eV)[20].

In order to evaluate the photocatalytic effectiveness of the insoluble complexes **1** ~**3**, the photocatalytic degradation of ethylene blue (MB) aqueous solution was performed at ambient temperature. Excitingly, complexes **1**~**3** exhibit good photocatalytic activities in the presence of H_2O_2 under a 300 W xenon lamp irradiation. As can be seen in Fig.5, the characteristic absorption peak of MB (665 nm) were gradually reduced with time increasing from 0 to 60 min. Besides, the changes in the C_t/C_0 plot of MB solutions versus irradiation time are shown in Fig.6 to clarify the photocatalytic results, wherein C_t is the concentration of the MB solutions at t time and C_0 is the concentration of the MB solutions at the beginning of irridiation. From Fig.6, the degradation ratio of MB reaches 17% without any photocatalyst, while it increases to 79%, 81% and 88%, respectively, when complexes **1**, **2** and **3** are added to the mixture as catalyst.

Further studies about the stability and reproducibility are also carried out shown in Fig.6b, and the results show that the catalytic activities of complexes **1**~**3** do not exhibit a significant decrease after four runs in the same photocatalytic tests (Table 3), which manifest that the complexes **1**~**3** as photocatalysts are very stable and possess good reproducibility.

We know that the efficiency of the photocatalyst is a function of the balance between charge separation, interfacial electron transfer, and charge recombination. In general, a narrow band gap leads to the ease of the charge separation, so the photocatalytic degradation rates of MB should follow the reverse

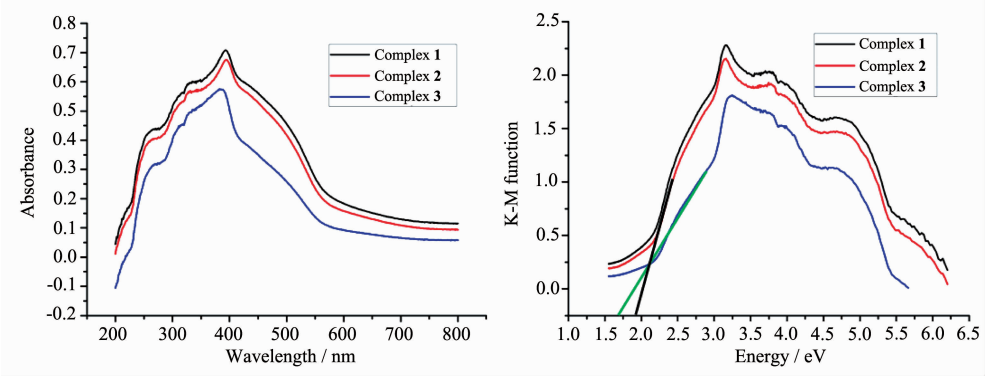

Fig.4 (a) UV-Vis absorption spectra of complexes **1**~**3**; (b) Kubelka-Munk-transformed diffuse reflectance of complexes **1**~**3**

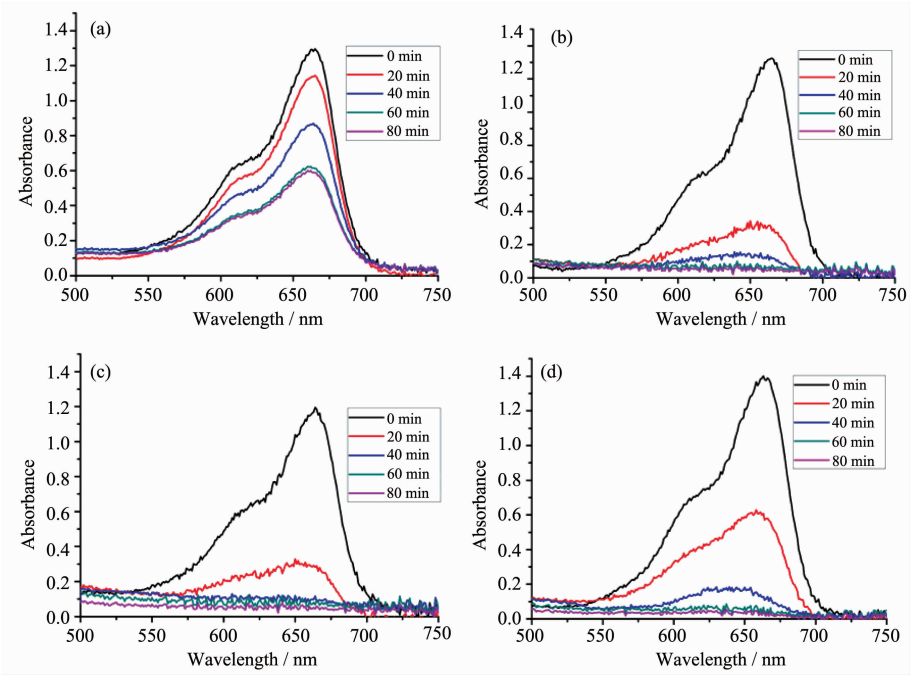

(a) without catalyst, (b) with complex **1**, (c) with complex **2**, (d) with complex **3**

Fig.5 Absorption spectra of the solution of MB

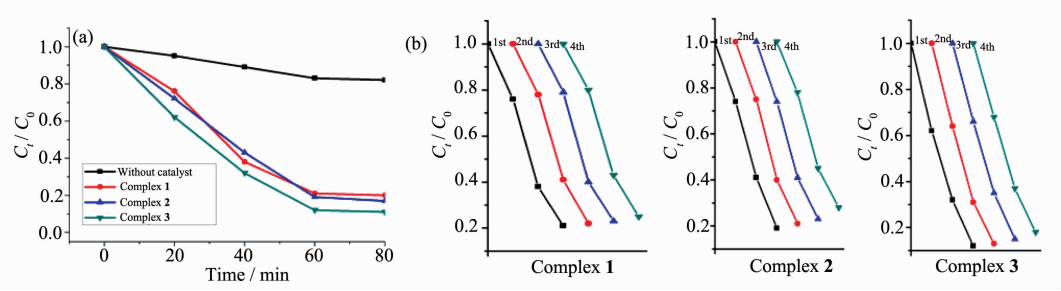

Fig.6 (a) Photodegradation of MB with complexes **1~3**; (b) Recycling experiments using complexes **1~3** for the photocatalytic degradation of MB solution

Table 3 Recycling experiments using complexes 1~3 for the photocatalytic degradation of MB solution

Complex	Degradation rate of MB / %		
	1	**2**	**3**
1st run	79.1	81.3	88.6
2nd run	78.8	81.1	87.2
3rd run	77.4	77.7	85.7
4th run	75.5	76.7	82.8

order of band gaps of the complexes. As calculated, the band gaps of complexes **1~3** are 1.85, 1.92 and 1.65 eV, respectively. The E_g of **1~3** follows the sequence: **3**<**1**≈**2**, and the reverse sequence of band gaps agrees with the degradation rates of MB. In addition, the stabilities of these three complexes are investigated by measuring the powder PXRD patterns after photocatalytic reactions (Fig.3). The PXRD patterns are consistent with those of the original ones, which confirm that these complexes keep their skeleton well after the photocatalytic process. The photocatalytic research result indicates that complexes **1~3** are good

photocatalytic catalyst in decomposing MB in the presence of H_2O_2 and may have possible application in decomposing other dyestuff.

3 Conclusions

In summary, an asymmetric triazolate derivative, 2-(5-(pyridin-3-yl)-1*H*-1,2,4-triazol-3-yl) pyrazine (Hptp), was employed to achieve three novel complexes $[Cd_2(ptp)_2(SO_4)(H_2O)_2]_n$ (**1**), $[Zn(ptp)_2(H_2O)_2]$ (**2**) and $[Cd(ptp)_2(H_2O)_2]$ (**3**). The structures of these complexes were characterized by single-crystal X-ray diffraction, powder X-ray diffraction, elemental analyses and infrared spectra. The photocatalytic experiment result indicates that complexes **1**~**3** are good candidates as photocatalysts in decomposing MB in the presence of H_2O_2.

References:

[1] Stock N, Biswas S. *Chem. Rev.*, **2012**,112:933-969

[2] White K A, Chengelis D A, Gogick K A, et al. *J. Am. Chem. Soc*., **2009**,**131**:18069-18071

[3] Alezi D, Belmabkhout Y, Suyetin Mil, et al. *J. Am. Chem. Soc*., **2015**,137:13308-13318

[4] Brozek C K, Dinc M. *J. Am. Chem. Soc*., **2013**,**135**:12886-12891

[5] Wang F, Liu Z S, Yang H, et al. *Angew. Chem. Int. Ed.*, **2011**,**50**:450-453

[6] Saha S, Das G, Thote J, et al. *J. Am. Chem. Soc*., **2014**,**136**:14845-14851

[7] Kim D, Whang D R, Park S Y. *J. Am. Chem. Soc*., **2016**, **138**:8698-8701

[8] Zheng B, Bai J, Duan J, et al. *J. Am. Chem. Soc*., **2011**,**133**:748-751

[9] WANG Hui(王慧), GAN Guo-Qing(甘国庆), QU Yang(瞿阳), et al. *Chinese J. Inorg. Chem.* (无机化学学报), **2012**, **28**:1217-1221

[10]Cheng J J, Chang Y T, Wu C J, et al. *CrystEngComm*, **2012**,**14**:537-543

[11]Shi X, Wang X, Li L, et al. *Cryst. Growth Des*., **2010**,**10**:2490-2500

[12]Xu Z, Wang Q, Li H, et al. *Chem. Commun*., **2012**,**48**:5736-5378

[13]Xu Z, Meng W, Li H, et al. *Inorg. Chem*., **2014**,**53**:3260-3262

[14]Xu Z, Li H, Li A, et al. *Inorg. Chem. Commun*., **2013**,**36**:126-129

[15]Pan J, Jiang F L, Wu M Y, et al. *Cryst. Growth Des*., **2014**,**14**:5011-5018

[16]XU Zhou-Qing (徐周庆), WANG Xiao-Ning (王晓宁), LI Hui-Jun (李慧军), et al. *Chinese J. Inorg. Chem*. (无机化学学报), **2016**,**32**:1223-1230

[17]Sheldrick G M. *SHELXS*-97, *Programs for X-ray Crystal Structure Solution*, University of Göttingen, Germany, **1997**.

[18]SADABS, Bruker AXS Inc., Madison, WI, **2004**.

[19]Meng W, Xu Z Q, Ding J, et al. *Cryst. Growth Des*., **2014**, **14**:730-738

[20]Silva C G, Corma A, García H. *J. Mater. Chem*., **2010**,**20**:3141-3156